

Excerpt from

FRACTAL SPACE-TIME AND MICROPHYSICS: Towards a Theory of Scale Relativity

L.Nottale

©WorldScientific, 1993, pp. 307-321.

(misprints corrected and note added, 1 February 2006)

Chapter 7

PROSPECTS

7.2. Beyond Chaos.

At the end of Section 5.7, we arrived at the conclusion that a Markov-Wiener process plays the fundamental role of a transformation allowing one to go reversibly from classical to quantum and from quantum to classical laws. However the completely deterministic “purely classical” world and the completely undeterministic “purely quantum” world may be viewed as the extremities of a full spectrum in the complexity of Nature: We, indeed, now know that “deterministic” chaos exists in several situations, some of which were previously considered as archetypes for totally predictable systems. One of the most impressive example is the recent suggestion by Laskar that the inner Solar System is chaotic with an inverse Lyapunov exponent as low as 5 Myr.

The discovery of chaos, which is now defined as the extreme sensibility to variation in initial conditions (this is often described by an exponential divergence of trajectories in phase space, $\delta x = \delta x_0 e^{t/\tau}$, where $1/\tau$ is the so-called Lyapunov or characteristic exponent³⁰), may be attributed to Poincaré.³¹

Chaos is relevant in a huge variety of natural systems (see, e.g., the series of popular papers in Refs. 32 and 40: celestial mechanics, fluid mechanics and turbulence, weather, population dynamics, evolution, ecology, mathematics, economics, dynamics of chemical reactions...). Although a large number of various methods of analysis has been coined to describe the development of chaos (strange attractors, fractal and information dimensions, entropy, characteristic exponents, catastrophe theory...), all of them have up to now struck against the unpassable barrier of unpredictability at large time scales. However, in many systems where chaos arises, spatial and temporal structures seem also to arise: they are observed experimentally (regularity of the distribution of planets, satellites and asteroids in the Solar System, spatial and temporal structures in the climate, biological structures, Belousov-Zhabotinskii reaction in chemistry, Taylor-Couette flow...); these structures are in some few cases found or confirmed in numerical simulations, but very rarely understood or predicted from a fundamental theory.

We suggest in the present section a general method for attacking these problems: this method is efficient precisely when other methods fail, i.e., for very large time scales (compared to the “chaos time” τ). We shall see that it naturally generates spatial and temporal structures. This will be exemplified by its application to the problem of the Solar System.

Prediction beyond unpredictability.

The method is based on the formalism presented in Sec. 5.6, which is an extension of Nelson's stochastic formalism. It is written in a compact form thanks to the introduction of complex variables; the main new point is that we have demonstrated that the fundamental equation of dynamics, written in terms of our new complex time derivative operator \hat{d}/dt ,

$$\mathbf{F} = m \frac{\hat{d}^2}{dt^2} \mathbf{x} \quad ,$$

becomes Schrödinger's equation. But consider the basic hypothesis of the formalism: the trajectory slopes are broken at any point of the space, this breaking being described by an Einstein-Wiener process of diffusion, as is done for the description of Brownian motion. Consider now chaotic

trajectories in the plane. We place ourselves in the reference frame of a first trajectory, say $(x_1 = 0, y_1 = a t)$. Then consider a second trajectory which is exponentially divergent with respect to the first one (we assume a unique Lyapunov exponent for simplicity): $x = \delta x e^{t/\tau}, y = a t + \delta y e^{t/\tau}$. Then we get the relation

$$y = \frac{\delta y}{\delta x} x + a \tau \ln \frac{x}{\delta x} .$$

Such a trajectory (typically in $x + \ln x$) is shown in Fig. 7.3 in the plane (x,y) , for various time scales. For very large time scales, i.e., with *resolution* $\gtrsim \tau$, it becomes non-differentiable at the origin, with different backward and forward slopes, and looks like trajectories arising from a diffusion process or from particle collision. For Lyapunov exponents different in x and y , one gets a power law, with also a point of broken slope at the origin when seen at large time scale. Now, in case of developed chaos, the small perturbation $(\delta x, \delta y)$ fluctuates and the divergence between possible trajectories described in Fig. 7.3 occurs at any of their points: for $\Delta t \gg \tau$, the trajectories become describable to a good approximation by non-differentiable and fractal paths.

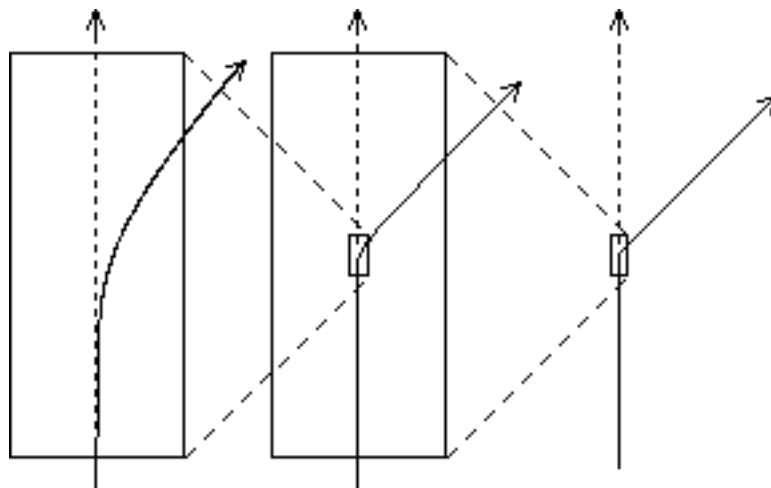


Figure 7.3. Schematic representation of the relative evolution of two initially close trajectories seen at three different time scales, in the case of chaotic motion.

Let us give another example. Consider one of the archetypes of chaotic behaviour, the so-called logistic map of population dynamics,

$$x_{t+1} = \lambda x_t (1 - x_t) ,$$

which may be iterated for a discrete time t . For $\lambda = 4$, the behaviour becomes completely chaotic and the values of x fill the interval $[0,1]$, as shown in Fig. 7.4. There too, it is immediately clear that the motion on the line Ox resembles closely that of a particle subjected to random kicks, with different velocities before and after the “kick”.

More generally, consider a system subject to developed chaos. For time scales large with respect to the inverse maximum Lyapunov exponent (i.e., beyond the time scale after which predictability of orbits is lost), we can replace deterministic trajectories by families of potential trajectories, and then the concept of definite positions by that of a *probability density*.

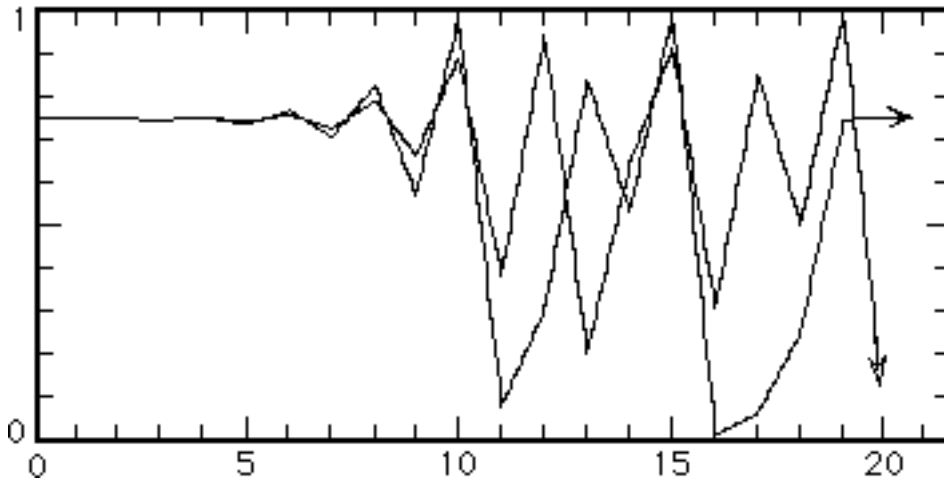


Figure 7.4. Illustration of high sensibility to initial conditions in the “logistic map”.

This leads one to describe the effect of chaos in a stochastic way by a diffusion process. Such an idea is not new in itself (see e.g. Ref. 61). The new element that we suggest to add in the description is the *explicit* introduction of the non-differentiability in terms of different *backward and forward velocities*.

So our method consists in assuming that, for large time scales, the evolution of the virtual trajectories can be described by a Wiener process, and replacing in the basic differential equations the time derivative by our complex time derivative operator (see Sec. 5.6). In other words, this means that we set a *principle of correspondence* for classical chaotic equations. When these classical equations are deduced from a Lagrangian formulation, the new equations will be Schrödinger-like, and the solutions quasi-

quantum (with a different interpretation: the full behaviour of quantum mechanics can be recovered only if one assumes the space-time to be *non-differentiable down to the smallest scales*; here this is only a large time scale approximation, since when coming back to small time scales one recovers differentiable predictable trajectories).

It is known that quantum mechanics naturally yields structures: the existence of well-defined boundary conditions for some variables results in the quantization of the conjugate variables. One may expect the same behaviour from the theory which is outlined here. Let us exemplify this by applying our method to celestial mechanics, namely, to the old problem of the regularity of planets in the Solar System.

“Quantization” of the Solar System.

The existence of regularities in the distribution of planets in the Solar System was recognized long ago. This was Kepler's main motivation in his search for planetary laws. The Titius-Bode “law” ($r_n = 0.4 + 0.3 \times 2^n$) was the first empirical attempt at describing these regularities, and was followed by several other proposals.³³⁻³⁵ The discovery of similar structures in the distribution of the satellites of the great planets led to a revival of interest for such studies, and to the hope that indeed a physical mechanism was at work; such a mechanism was searched for by most authors in the formation conditions.³⁶ It was however suggested by Hills³⁷ that this regularity may arise from a dynamical evolution relaxation (see Nieto³³).

The discovery by Laskar³⁸ that the inner planetary system (telluric planets) is chaotic, with a very short inverse Lyapunov exponent of $\tau \approx 5$ Myr, and its recent confirmation by independent studies³⁹ sets the question in a completely renewed way. The position of planets can no more be predicted from usual celestial mechanics for time scales larger than ≈ 100 Myr. But several arguments, among which the maintenance of life on Earth since $\approx 3.5-4$ Gyr, show us from experience that the Solar System, though chaotic, is nevertheless confined.⁴⁰ Let us apply here our new method for tackling this problem: we shall see that it allows us to predict the preferential positions of planets and leads to the suggestion that these structures can arise from large time scale effects of dynamical chaos.

The impossibility of following individual orbits for $t \gtrsim 100$ Myr forces us to jump to a probabilistic description. The planet position is now characterized by a probability density ρ (which applies to *potential* orbits) rather than by well-defined variables. Once the chaos developed, the various future or past potential trajectories evolve following a diffusion process, characterized by some diffusion coefficient \mathcal{D} . We describe this diffusion by a Markov-Wiener process $\xi(t)$ (i.e. the $d\xi(t)$ are Gaussian with mean zero, mutually independent and such that $\langle (d\xi)^2 \rangle = 2\mathcal{D}dt$) as in the formalism of Sec. 5.6. Let us recall once more the main steps of the demonstration.

Mean forward and backward derivatives⁴¹, d_+/dt and d_-/dt , are introduced which, once applied to the position vector \mathbf{x} , yield *forward and backward mean velocities*, $\frac{d_+}{dt}\mathbf{x}(t) = \mathbf{b}_+$ and $\frac{d_-}{dt}\mathbf{x}(t) = \mathbf{b}_-$. This describes the fact that, at the time scales considered, the trajectories are broken at any of their points (i.e. fractal). From these quantities we introduce a complex velocity

$$V = \mathbf{V} - i \mathbf{U} = \frac{\mathbf{b}_+ + \mathbf{b}_-}{2} - i \frac{\mathbf{b}_+ - \mathbf{b}_-}{2}$$

and a complex derivative operator

$$\frac{d}{dt} = \frac{d_y}{dt} - i \frac{d_u}{dt} = \frac{1}{2} \left(\frac{d_+ + d_-}{dt} - i \frac{d_+ - d_-}{dt} \right)$$

which is given by

$$\frac{d}{dt} = \left(\frac{\partial}{\partial t} - i \mathcal{D} \Delta \right) + \mathbf{V} \cdot \nabla .$$

The real part \mathbf{V} of V is identified with the classical velocity in the differentiable case, while its imaginary part \mathbf{U} is non-zero only in the non-differentiable case. Now, since we deal with a Markov process, the probability density verifies the forward and backward Fokker-Planck equations, from which the equation of continuity and the following expression for \mathbf{U} may be derived:⁴¹

$$\mathbf{U} = \mathcal{D} \nabla \ln \rho .$$

We conjecture that Newton's equation of dynamics still holds in terms of our new complex variables

$$F = m \frac{d}{dt} V.$$

As seen in Sec 5.6, the action principle may also be re-expressed in terms of complex variables: this leads to the above form of Newton's equation and to the result that V is also a gradient. We thus introduce a new quantity S such that $V = 2 \mathcal{D} \nabla S$ and define a complex function ψ which is related to our complex velocity :

$$\psi = \sqrt{\rho} e^{iS} \Rightarrow V = -2 i \mathcal{D} \nabla (\ln \psi).$$

When the force F derives from a potential, $F = -\nabla U$, as is the case for gravitation, the equation of motion writes

$$\nabla U = 2 i \mathcal{D} m \frac{d}{dt} (\nabla \ln \psi).$$

Replacing the complex derivative operator by its expression finally gives

$$\mathcal{D}^2 \Delta \psi + i \mathcal{D} \frac{\partial}{\partial t} \psi - \frac{U}{2m} \psi = 0 \quad (7.2.1a)$$

up to an arbitrary phase factor. Take $\mathcal{D} = \hbar/2m$, and this becomes Schrödinger's equation, as shown in Sec. 5.6. The hereabove system is a reexpression of stochastic quantum mechanics,⁴¹ but also a generalization: assume that one has been able to characterize some chaotic system for large time scale by a constant diffusion coefficient \mathcal{D} , then (7.2.1) is a quasi-quantum equation for such a system, which is expected to yield structures (i.e., peaks of probability) once the boundary conditions are prescribed.

Let us apply this method to the Solar System. Consider a planet (more generally a test particle) in the field of the Sun, $U = -GmM/r$, and in the collective field of an ensemble of planets (more generally of particles), and assume that this system is chaotic. Our conjecture is that the effect of chaos on large time scales can be summarized by a Brownian motion

process of diffusion coefficient \mathcal{D} . Assume moreover that we deal with a stationary motion with conservative energy $E \equiv 2 i \mathcal{D} m \partial/\partial t$ (the time-independent Schrödinger equation may also be obtained directly by setting $V=0$, see Nelson⁴¹). Equation (7.2.1a) becomes

$$\mathcal{D} \Delta \psi + \left[\frac{E}{2 m \mathcal{D}} + \frac{G M}{2 \mathcal{D} r} \right] \psi = 0. \quad (7.2.1b)^1$$

The equivalence principle suggests that \mathcal{D} must be independent of m . This equation is similar to the Schrödinger equation for the hydrogen atom,^{42,43} up to the substitutions $\hbar/2m \rightarrow \mathcal{D}$, $e^2 \rightarrow GmM$, so that the natural unit of length (which corresponds to the Bohr radius) is

$$a_0 = \frac{4 \mathcal{D}^2}{G M}. \quad (7.2.2)$$

We thus find that the energies E of planets are given by²

$$E_n = - \frac{G^2 m M^2}{8 \mathcal{D}^2 n^2}, \quad n = 1, 2, 3, \dots,$$

and that the density of probability of their distances to the Sun are confined to well defined regions given by the square of the well-known radial wave function^{42,43} of the hydrogen atom (see Sec. 4.1). We also expect angular momenta to scale as $L = 2m\mathcal{D}l$, with $l = 0, 1, \dots, n-1$. This means that, unlike the case of quantum mechanics, E/m and L/m are quantized rather than E and L . The average distance to the Sun and the eccentricity e are given in terms of the two quantum numbers n and l by the following relations:

$$a_{nl} = \left\{ \frac{3}{2} n^2 - \frac{1}{2} l(l+1) \right\} a_0, \quad (7.2.3)$$

¹ A misprint in the published version has been corrected (the denominator $2 m \mathcal{D}$ was lacking under the energy term) and an equation number has been added.

² A misprint in the published version has been corrected (G^2 instead of G).

$$e^2 = 1 - \frac{l(l+1)}{n(n-1)} . \quad (7.2.4)^3$$

In order to compare these results with the actual Solar System, one must first note that the inner (Mercury to Mars) and outer (Jupiter to Neptune and/or Pluto) planetary systems are characterized by two different inverse Lyapunov exponents, $\tau_{\text{int}}=5$ Myr and a still unknown τ_{ext} , perhaps as high as 1 Gyr.^{44,45} That they must be treated as two different systems is also suggested by many other arguments, such as their different chemical compositions and mass distributions.

Consider first the eccentricities. Even the largest eccentricities (Pluto, $e^2=0.065$; Mercury, $e^2=0.042$) correspond to a good approximation to $l=n-1$. This will be further discussed hereafter. We may then compare the observed values of semi-major axes of the planets to our prediction (Eq. 7.2.5), $a = (n^2+n/2)a_0$. This is only a *one-parameter* relation⁴ (the slopes for the inner and outer systems are themselves related), since *we predict the ordinate at origin to be zero*. This prediction is very well verified for the two systems. We find Mercury, Venus, the Earth and Mars to take respectively the ranks 3, 4, 5, and 6 in the inner system and Jupiter, Saturne, Uranus, Neptune, and Pluto the ranks $n = 2, 3, 4, 5, 6$ in the outer system. With these values, the regression lines are (in units of A.U.)

$$\sqrt{a_{\text{int}}} = -0.015 + 0.199 \sqrt{(n^2+n/2)} ,$$

$$\sqrt{a_{\text{ext}}} = -0.066 + 1.035 \sqrt{(n^2+n/2)} ,$$

so $a_{\text{int}}(0) = 2 \times 10^{-4}$ A.U. and $a_{\text{ext}}(0) = 4 \times 10^{-3}$ A.U., which are a fair confirmation of our prediction. Assuming them to be strictly zero, we get

³ Subsequent works have proved this relation to be wrong. It was derived by using incorrectly a classical expression for the eccentricity in which the quantum mechanical expression has been inserted. Actually the states obtained in spherical coordinates are characterized by given values of E, L and L_z , so that the eccentricity is undefined in this case. For obtaining a quantum theoretical prediction for the eccentricity, one must use parabolic coordinates, which define states characterized by given values of E, L_z and A_z , where A is the Runge-Lenz vector. This is a conservative quantity which is specific of the Kepler problem, whose modulus is precisely the eccentricity. By taking the axis z along the major axis, one therefore derives a quantization formula for the eccentricity which reads $e = k/n$, where $k < n$ is an integer (See e.g. Da Rocha D. & Nottale L., 2003, *Chaos Solitons and Fractals*, 16, 565 (arXiv:astro-ph/0310036) "Gravitational structure formation in scale relativity").

⁴ A misprint in the published version has been corrected (one-parameter instead of two-parameter).

average slopes $\sqrt{a_{o \text{ int}}} = 0.195 \pm 0.0022$ and $\sqrt{a_{o \text{ ext}}} = 1.014 \pm 0.016$. Their ratio is 5.2 ± 0.1 . (Note that the value of the inner slope mainly reflects the fact that the rank of the Earth is $n = 5$).

Two additional remarkable results are obtained: (i) the central peak of the asteroid belt (2.7 A.U.) agrees remarkably well with $n = 8$ of the inner system, and the main peak at 3.15 A.U. with $n = 9$; (ii) Mars' position is also in very good agreement with $n = 1$ of the *external* system. Including them yields improved slopes $(\sqrt{a_{o \text{ int}}}) = 0.195 \pm 0.0017$ and $(\sqrt{a_{o \text{ ext}}}) = 1.014 \pm 0.012$. These results are illustrated in Fig. 7.5.

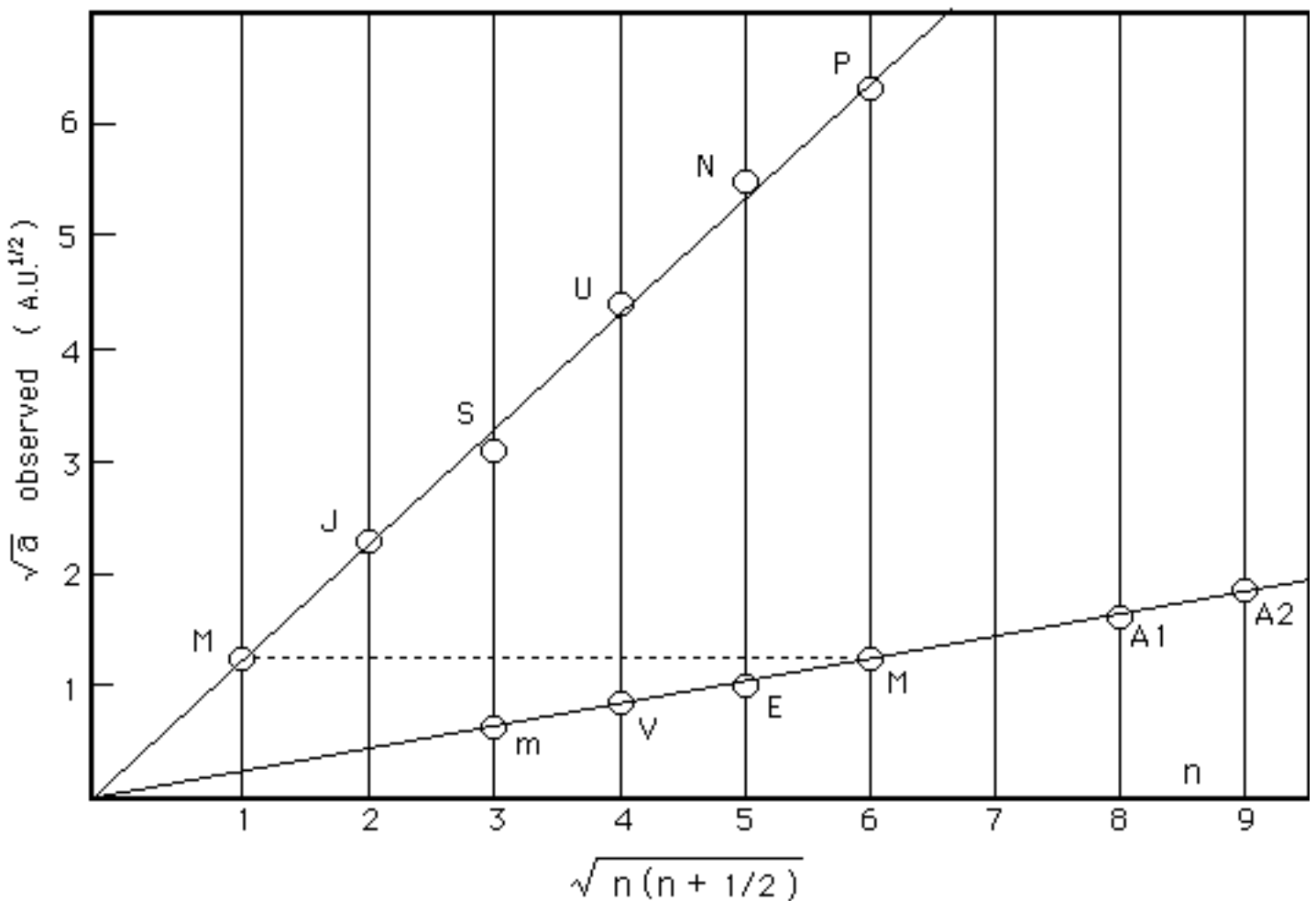


Figure 7.5. Comparison of the observed average distances of planets to the Sun with our prediction (see text). The lines shown are least-square regression lines. A1 and A2 stand for the two main peaks in the distribution of asteroids in the asteroid belt.⁵

⁵ Note the theoretical prediction, apparent in this figure, of the two probability peaks $n = 1$ (≈ 0.043 AU) and $n = 2$ (≈ 0.17 AU) in which no large planet lies in our own inner Solar System, but whose

Note also the agreement of Pluto with the outer relation: this may seem to be at variance with its particular orbit and the recent discovery that its motion is chaotic with a Lyapunov $1/20$ Myr;⁴⁶ however it has been argued that this chaos arises from resonances within resonances and that this can limit the extent of Pluto's wandering.⁴⁷ We shall see that indeed Pluto is “anomalous” in terms of angular momentum, while our results show that it is not so in terms of energy. In this respect, it is also noticeable that Neptune and Pluto, both of which strongly disagreed with the *three*-parameter Titius-Bode law, now both agree with our two-parameter relation: moreover, as will be seen later, one may have the hope to see this relation become a full totally constrained prediction, when the slopes are precisely predicted from the Lyapunov exponents (or some other characteristic of the chaotic dynamics).

The agreement between observations and predictions are tested in two ways. We may compute $(a_{\text{pred}} - a_{\text{obs}})/a_{\text{obs}}$ for each planet. This is shown in column 5 of Table 1. The only difference larger than $\approx 6\%$ is Saturn (12 %). The average relative difference is 3.4% in the inner system and 2.6% (Saturn excluded) or 4.3% (Saturn included) in the outer system. These numbers are certainly indicative of the natural irreducible fluctuations of the distance which are expected from our analysis: this is anyway a remarkable confinement around the mean values, perhaps too good when compared with the theoretical dispersion in the probability densities. At the end of this section, we shall consider some improvements of the method which could help us to understand such narrow fluctuations. If we take our results at face value, the Earth would presently be in one of its closest approach to the sun (4%).

Another test consists in checking the difference with the quantized values n . Let us introduce δn such that $(n + \delta n)^2 + (n + \delta n)/2 = a_{\text{obs}}/a_0$. To lowest order in δn it is given by

$$\delta n = \frac{a_{\text{obs}}/a_0 - n(n + 1/2)}{2(n + 1/4)} .$$

existence has been later supported by the discovery of extrasolar planets (since 1995): more than 30 exoplanets have been found to lie in the $(n = 1)$ peak (by the end of 2005).

The values of δn for the various planets are given in column 6 of Table 1.

The statistical nature of our predictions is more clearly visible in this indicator, which reaches 0.18 at the maximum difference.

Planet (1)	n (2)	a_{obs} (UA) (3)	a_{pred} (AU) (4)	$\delta a/a$ (5)	δn (6)	e (7)	δl (8)
Mercury	3	0.387	0.399	+0.031	-0.065	0.206	0.051
Venus	4	0.723	0.684	-0.054	+0.098	0.007	0.00008
Earth	5	1	1.045	+0.045	-0.139	0.017	0.0006
Mars	6	1.523	1.483	-0.026	+0.053	0.093	0.024
-	7	-	1.996	-	-	-	-
Aster.1	8	2.7	2.586	+0.043	+0.140	-	-
Aster.2	9	3.15	3.251	+0.030	-0.073	-	-
Mars ⁶	1	1.523	1.542	+0.012	-0.008	0.093	0.00000
Jupiter	2	5.20	5.14	-0.012	+0.013	0.048	0.0008
Saturn	3	9.57	10.79	+0.126	-0.183	0.054	0.0036
Uranus	4	19.28	18.51	-0.040	+0.088	0.051	0.0044
Neptune	5	30.14	28.27	-0.062	+0.173	0.005	0.00006
Pluto	6	39.88	40.09	+0.005	-0.017	0.256	0.178

Table 1.

Let us now come back to angular momenta. From the now known values of n for the various planets, one may compute the difference with the expected quantized number l . We set $l = n - 1 + \delta l$, and find from Eq. (7.2.4) (to lowest order in δl)

$$\delta l = \frac{n(n-1)}{2n-1} e^2 .$$

⁶ In further works, the $n = 1$ 'orbital' of the outer Solar System has been better identified with the whole inner system itself (see e.g. Nottale, L., Schumacher, G., Gay, J., 1997, Astron. Astrophys., 322, 1018, <http://wwwusr.obspm.fr/~nottale/arA&A322.pdf>).

The δ/l values are given in column 8 of Table 1. They are remarkably small (some 1‰ or less), except in one case, Pluto, for which the difference amounts to 0.18: indeed the orbit of Pluto is known to be partly determined by its strong 3:2 resonance with Neptune. Concerning the asteroid belt, there is a large spread of observed eccentricities from 0 to ≈ 0.4 , which may be shown to arise from Jupiter's perturbation⁴⁸ (more generally from the four Jovian planets). For $n = 8$ (main asteroid belt), the second angular momentum state is $l = 6$, which gives $e = 0.5$. There is indeed a population of asteroids with eccentricities around this value.

Our method also sheds new light on one of the long standing problems concerning the Solar System, namely that of the distribution of angular momentum. Jupiter owns 62% of the angular momentum of the Solar System and Saturn 25%. We have found that the angular momentum over m is quantized, rather than the angular momentum itself. So the distribution of angular momentum mainly reflects that of mass, hence implying the domination of Jupiter and Saturn. (The origin of the distribution of mass comes under the theories of formation of the solar system, which are outside the scope of the present work⁷). In contrast, the method in its present form does not allow us to understand the alignment of angular momentum vectors (i.e. the nearly plane character of the Solar System).

Concerning asteroids in the main belt, one may now reach a good understanding of their distribution. First our approach brings new elements for understanding the absence of a large planet there: the zone where the belt lies, even though it corresponds to the maxima of probability density for the inner system, also corresponds to a *minimum* in the outer system. The region between Mars and Jupiter is where the two systems overlap (see Fig. 7.5). While Mars, being in a probable zone in both systems, is expected to have a remarkably stable orbit, (the mean predicted distance is 1.51 A.U., the observed distance 1.52 A.U.), this is not the case of the belt region, for which the tendencies are opposite. Then most of the matter of the primordial nebula situated between the $n = 1$ and $n = 2$ orbitals of the outer system could have drifted towards what are now Mars and Jupiter: this may

⁷ We have reconsidered this conclusion in further works, see e.g. Nottale, L., Schumacher, G., Gay, J., 1997, *Astron. Astrophys.*, 322, 1018, <http://www.usr.obspm.fr/~nottale/arA&A322.pdf>.

explain why the total mass of asteroids is far smaller than a planet mass. However, peaks of probability occur at $n = 7, 8, 9$ and 10 between Mars and Jupiter, in terms of the inner system. Why are they not all filled? This is due to the small time scale dynamical chaos⁴⁸: the orbitals $n = 7$ and $n = 10$ coincide with the resonances 1:4 and 2:3 with Jupiter (see Fig. 3.4 of Sec. 3.2). So one may hope to understand the existence and full distribution of asteroids as a combination of the effect of large time scale chaos (implying peaks of probability at 2.59 and 3.25 U.A.⁸) and of small time scale chaos due to the resonant action of Jupiter resulting in the formation of the Kirkwood gaps.⁴⁸

All the above results have been obtained without specifying any expression for the diffusion coefficients \mathcal{D} of the inner and outer systems, which were left as free parameters (and then fitted in Fig. 7.5). Is it possible to get estimates for them, in particular to relate them to the calculated Lyapunov exponents ?

The problem is that the chaotic behaviour discovered by Laskar concerns essentially the eccentricities and inclinations, while nothing is *a priori* known concerning the semi-major axes. The distance at time t of two orbits initially separated by δx_0 is $x = \delta x_0 e^{t/\tau}$, where $1/\tau$ is the Lyapunov exponent which characterizes the chaotic behaviour. Predictability of the planet position is completely lost when $x \approx a$. However this does not mean that predictability of the mean distance a of the planet to the sun is yet lost. Loss of information on the precise position is first indicated by a loss of information on the angle (see e.g. the time evolution of orbits in Ref. 44) This occurs when $\delta x_0 e^{t/\tau} \approx a$. Beyond this point, the divergence may begin to contribute to the loss of the information on the average distance to the Sun. It is completely lost after some number k of turns at a time T given by $\delta x_0 e^{T/\tau} \approx 2k\pi a$. If one *assumes* that the drift on 1 radian remains of the order of δx_0 , one gets $2\pi k \approx a/\delta x_0$ and then $\delta x_0 \approx a e^{-T/2\tau}$. This very rough estimate, which corresponds to an inverse Lyapunov exponent for semi-major axes (i.e., energy) twice that of other orbital elements, should be considered as a lower limit only.

⁸ Misprint corrected: 3.25 AU instead of 4.25 AU in the published version.

The diffusion coefficient is given by $\mathcal{D} = U/\nabla \ln \rho$. The probability of presence for $l=n-1$ (corresponding to quasi circular states $e^2 \approx 0$ as observed for planets in the solar system, see hereafter) writes

$$P_n(r) = \frac{1}{(2n)!} \frac{8}{n^3} \left(\frac{2r}{na_0}\right)^{2n-2} e^{-2r/na_0}$$

so that $(\nabla \ln \rho)^{-1} \approx na_0/2 \approx a/2n$, while $U \approx \langle \frac{\delta x_0}{2\tau} e^{t/\tau} \rangle \approx \frac{\delta x_0}{2T} e^{T/\tau}$. Setting $R=a/\delta x_0$, we finally get a rough estimate for the diffusion coefficient:

$$\mathcal{D} \approx \frac{1}{8n} \frac{R}{\ln R} \frac{a^2}{\tau} .$$

From Eq. (7.2.2), it is also given by $\mathcal{D} = \frac{1}{2}\sqrt{GMa_0}$. From Eq. (7.2.3), $a = (n^2+n/2)a_0$ for quasi-circular states ($l=n-1$). We may then estimate the slope of the linear relation expected between \sqrt{a} and $\sqrt{(n^2+n/2)}$:

$$\sqrt{a_0} = \frac{1}{\langle n \rangle} \left(4\tau \sqrt{GM} \frac{\ln R}{R} \right)^{1/3} . \quad (7.2.5)$$

Using Kepler's third law ($T^2/a^3 = cst$) allows us to write this result in still another form in terms of the planet period T :

$$\frac{\tau}{T} = \frac{1}{8\pi} \frac{R}{\ln R} .$$

Let us finally attempt to compare our estimate of the slope (7.2.5) with the observed one in the inner system, $\sqrt{a_0} = 0.195$ (U.A.)^{1/2} = $7.5 \cdot 10^5$ cm^{1/2}. Our estimate depends on the parameter $R = a/\delta x_0$, then on the value of the basic perturbation δx_0 . This does not correspond here to a measurement uncertainty, but to the irreducible fluctuations of the positions of the planets due to internal and/or external effects. The main effect comes from the interaction with asteroids.⁴⁵ It has been estimated that, in order to keep a precision $R^{-1} = 10^{-10}$, about 40 asteroids were to be included in the motion equations, and several hundreds at 10^{-12} precision.⁴⁵ The asteroid trajectories being themselves chaotic, we may estimate the irreducible perturbation to be such that $R = 10^{10 \pm 1}$. With $\tau_{\text{int}} = 5$ Myr and $\langle n \rangle = 4.5$ for the inner solar system, Eq. (7.2.5) yields

$$\sqrt{a_o} = (5.3^{+6.1}_{-2.8}) \times 10^5 \text{ cm}^{1/2} ,$$

which is compatible with the observed value. The diffusion coefficient is estimated to be $\mathcal{D} \approx 10^{19 \pm 1} \text{ cm}^2 \cdot \text{s}^{-1}$, to be compared with $\mathcal{D}_{\text{obs}} = \frac{1}{2} \sqrt{GM a_o} = (4.34 \pm 0.09) \times 10^{18} \text{ cm}^2 \cdot \text{s}^{-1}$. But this result should not be taken too seriously, because of all the uncertainties in its derivation. The large final error on the theoretical estimate (7.2.5) still allows the inverse Lyapunov exponent for semi-major axes to be 10 times its estimated minimal value, namely 100 Myr.

Moreover, it is quite possible that our method applies essentially to an earlier phase of the evolution of the Solar System, so that it would be irrelevant to relate the diffusion coefficient in Eq. (7.2.1) to Lyapunov exponents computed *from the present state* of the Solar System. The results of numerical simulations by Hills³⁷, Ovenden⁶² and Conway and Elsner⁶³ seem to support this view: starting from random initial conditions of model planetary systems, they find chaotic trajectories (the very irregular evolution of semi-major axes seen in Figs. 1, 2, 4 of Ref. 63 fairly agrees with our basic conjecture of fractality and non-differentiability), while systems placed initially in conditions similar to that of the present Solar System were shown to be very stable system, which maintained nearly circular orbits. Our results suggest that, on very large time scales, a planetary system can pass from the first type of system to the second one.

Anyway, the improvement of our approach needs a better understanding of the relation⁶¹ between the Lyapunov exponents, which describe the development of chaos, and the diffusion coefficients, which hopefully describe, in our approach, what happens *after* the limit of classical unpredictability. A promising method would consist in working with the Kolmogorov-Sinai entropy, which is itself related to Lyapunov exponents,³⁰ or with the algorithmic entropy recently introduced by Zurek.⁴⁹ However the Lyapunov exponent is presently calculated from numerical simulations, while a completely self-consistent approach would imply obtaining it also from the basic equations. These problems are left to future works.

Before closing this section, let us add a last comment: as already specified, even though our fundamental equation (7.2.1) is a quantum mechanical-like equation, its interpretation must be different from that of quantum mechanics. We know that the approximation of non-

differentiability is no more valid on small time scales, for which one recovers predictable and differentiable trajectories. So the (still open) problem is to understand how to connect the small time scale behaviour to the large time scale one, or in other words, how the probability densities obtained at large time scales influences the motion observed at small time scales.

7.2 References

30. Eckmann, J.P., & Ruelle, D., 1985, *Rev. Mod. Phys.* **57**, 617.
31. Poincaré, H., *Méthodes Nouvelles de la Mécanique Céleste* (Gauthier-Vilars, Paris, 1892).
32. Vivaldi, F., 1989, *New Scientist* (28 Oct.), p.46; Palmer, T., 1989, *New Scientist* (11 Nov.), p.56; Mullin, T., 1989, *New Scientist* (11 Nov.), p.52; May, R., 1989, *New Scientist* (18 Nov.), p.37; Scott, S., 1989, *New Scientist* (2 Dec.), p.53.
33. Nieto, M.M., *The Titius-Bode Law of Planetary Distances: Its History and Theory*. Pergamon Press. Oxford (1972).
34. Neuhäuser, R., & Feitzinger, J.V., 1986, *Astr. Astrophys.* **170**, 174. 35. Souriau, J.M., 1989, *Preprint CPT-89/P.2296*.
36. Brahic, A., (Ed.), *Formation of Planetary Systems*, (Cepadues Editions, Toulouse, 1982).
37. Hills, J.G., 1970, *Nature* **225**, 840.
38. Laskar, J., 1989, *Nature* **338**, 237.
39. Sussman, G., & Wisdom, J., 1991, in *Chaos, Resonances and Collective Dynamical Phenomena in the Solar System*, I.A.U. Symp. n°152, S. Ferraz-Mello, ed.
40. Murray, C., 1989, *New Scientist* (25 Nov.), p.61.
41. Nelson, E., 1966, *Phys. Rev.* **150**, 1079.
42. Landau, L. & Lifchitz, E., *Quantum Mechanics* (Mir, Moscow, 1967).
43. Messiah, A., *Mécanique Quantique*, (Dunod, Paris, 1959), p. 187.
44. Laskar, J., 1990, *Icarus* **88**, 266.
45. Laskar, J., 1991, in *Chaos, Resonances and Collective Dynamical Phenomena in the Solar System*, I.A.U. Symp. n°152, S. Ferraz-Mello, ed.
46. Sussman, G., & Wisdom, J., 1988, *Science* **241**, 433-437
47. Murray, C.D., 1986, *Icarus* **65**, 70.
48. Wisdom, J., 1987, *Icarus* **72**, 241.

49. Zurek, W.H., 1989, *Phys. Rev.* **A40**, 4731.
50. Kinoshita, T., 1989, *IEEE Trans. Instr. Meas.* **38**, 172.
51. Carruthers, P., 1989, *Int. J. Mod. Phys.* **A4**, 5587.
52. Thom, R., *Modèles Mathématiques de la Morphogenèse* (Union Générale d'Éditions, Paris, 1974).
53. Prigogine, I., & Stengers, I., *La Nouvelle Alliance* (Gallimard, Paris, 1979).
54. Gefen, Y., Mandelbrot, B., & Aharony, A., 1980, *Phys. Rev. Lett.* **45**, 855.
55. Clerc, J.P., Giraud, G., Laugier, J.M., & Luck, J.M., 1985, *J. Phys.* **A18**, 2565.
56. Le Méhauté, A., & Crépy, G., 1983, *Solid Stat. Ionics* **9/10**, 17
57. Le Méhauté, A., *Les Géométries Fractales* (Hermès, Paris, 1990).
58. Le Méhauté, A., 1990, *New J. Chem.* **14**, 207.
59. Le Méhauté, A., Héliodore, F., & Cottevieille, D., 1992, *Rev. Scien. Tech. Défense*, in the press.
60. *Engineering a Small World: From Atomic Manipulation to Microfabrication*, Special Section of *Science*, **254**, p. 1277-1335.
61. Lichtenberg, A.J., & Lieberman, M.A., *Regular and Stochastic Motion* (Springer-Verlag, New-York, 1983).
62. Ovenden, M.W., 1975, *Vistas in Astronomy* **18**, 473.
63. Conway, B.A., & Elsner, T.J., in *Long-Term Dynamical Behaviour of Natural and Artificial N-Body Systems* (Kluwer Acad. Pub. 1988), p. 3.